European Journal of Pharmaceutics and Biopharmaceutics 79 (2011) 142–149

Contents lists available at ScienceDirect

European Journal of Pharmaceutics and Biopharmaceutics

journal homepage: www.elsevier.com/locate/ejpb

Research paper

Cisplatin-loaded gelatin-poly(acrylic acid) nanoparticles: Synthesis, antitumor efficiency *in vivo* and penetration in tumors

Dan Ding [a], Zhenshu Zhu [a], Qin Liu [b], Jing Wang [a], Yong Hu [a], Xiqun Jiang [a,*], Baorui Liu [b]

[a] Department of Polymer Science & Engineering, Nanjing University, Nanjing, PR China
[b] The Comprehensive Cancer Center of Drum-Tower Hospital, Medical School of Nanjing University & Clinical Cancer Institute of Nanjing University, Nanjing, PR China

ARTICLE INFO

Article history:
Received 13 March 2010
Accepted in revised form 17 January 2011
Available online 25 January 2011

Keywords:
Polymer nanoparticles
Drug delivery
Antitumor
Cisplatin
Gelatin

ABSTRACT

Cisplatin (CDDP)-loaded gelatin-poly(acrylic acid) (GEL-PAA) nanoparticles were successfully prepared by polymerizing acrylic acid in the presence of gelatin in aqueous solution followed by incorporating CDDP into the formed GEL-PAA nanoparticles through polymer–metal complex formation of CDDP with carboxylic groups in the nanoparticles. The obtained nanoparticles had a spherical shape, with a mean size of about 100 nm, and high drug payload as well as stability. It is found that CDDP can be released from the nanoparticles in a sustained manner with a small initial burst release. *In vitro* cytotoxicity revealed that CDDP-loaded nanoparticles had similar cytotoxicity to free CDDP after 48 h co-incubation with human colorectal cancer cell line LoVo. *In vivo* antitumor activity indicated that the nanoparticle formulation was superior in anticancer effect to free CDDP on murine hepatic H22 tumor-bearing mice model through intraperitoneal (i.p.) administration and displayed a dose-dependent antitumor efficacy. Further, the penetration examination of the nanoparticles through tumor tissue revealed that the CDDP-loaded GEL-PAA nanoparticles could only affect the cells near the tumor vasculature after they entered into the tumor tissue.

1. Introduction

There is a substantial interest in developing biocompatible and biodegradable polymeric nanoparticles for both therapeutic and diagnostic purposes of cancers [1–3]. Recently, many types of nano-sized polymeric carriers, including polymer nanoparticles, polymeric micelles, polymer-modified liposomes and polymer–drug conjugates have been demonstrated to have the ability to efficiently enhance the antitumor efficacy of anticancer agents [4–7]. Furthermore, numerous polymeric nanoparticles have shown to significantly change the biodistribution of the loaded drug, reducing drug's side effects [8–10]. Particularly, it is widely known that nanoparticles are the vehicles beneficial for "passive" tumor targeting through the enhanced permeability and retention (EPR) effect, which can be taken as an advantage to effectively improve the drug concentration in tumor tissues after systemic administration (intravenous i.v., intraperitoneal i.p.) [11]. However, it is also found that some potential barriers hinder the deep permeation of drug-loaded nanoparticles through tumor tissue after they successfully reach the tumor. These include the abnormal tumor vessels, high interstitial fluid pressure and complex extracellular matrix (ECM) [12,13]. Thus, it is important to explore the ability of drug-loaded nanoparticles to efficiently penetrate in solid tumors to achieve great anticancer efficacy on tumor treatment. However, little work is focused on the penetration of nano-sized polymeric carriers in tumor except that Dreher et al. found that tumor penetration and accumulation of macromolecular drug carriers were relative to their size and molecular weight [14].

Cisplatin (*cis*-dichlorodiamminoplatinum (II); CDDP) is a widely used anticancer agent that has high antitumor activity. However, its clinical use is limited due to its severe side effects such as neurotoxicity, gastrointestinal disturbance, and acute nephrotoxicity [15]. In recent years, nano-scaled carriers have been reported to minimize side effects as well as enhance the accumulation and retention of CDDP in tumor tissues [16,17]. There are two strategies that are currently utilized to fabricate CDDP-encapsulated nanoparticles. One is physical entrapment of CDDP into amphiphilic block copolymeric nanoparticles, which suffers relatively rapid release of the loaded drug [18]. Another is chemically conjugating CDDP with nanoparticles consisting of carboxylic groups to form polymer–metal complex with a slower release profile [19]. Additionally, it has been pointed out that compared with CDDP physically entrapped nanoparticles, systemic administration of nanoparticles chemically conjugated with CDDP could achieve more superior anticancer effect over free drug [7,18].

* Corresponding author. Laboratory of Mesoscopic Chemistry and Department of Polymer Science & Engineering, College of Chemistry & Chemical Engineering, Nanjing University, Nanjing 210093, PR China. Tel.: +86 25 8359 7138; fax: +86 25 8331 7761.
E-mail address: jiangx@nju.edu.cn (X. Jiang).

0939-6411/$ - see front matter © 2011 Elsevier B.V. All rights reserved.
doi:10.1016/j.ejpb.2011.01.008

In the present study, we incorporated CDDP into gelatin-poly (acrylic acid) (GEL-PAA) nanoparticles through the interaction between platinum of CDDP and carboxylic groups in the nanoparticles. Gelatin is a proteinaceous biopolymer and has a long history of safe use in the fields of medicine and pharmaceutics due to its good biocompatible, biodegradable, and non-toxic properties [20,21]. In addition, the presence of PAA in nanoparticles, which provide plenty of carboxylic groups, offers dramatically high CDDP loading content. The feasibility of CDDP-loaded nanoparticles as a drug delivery system was examined by evaluating its *in vitro* cytotoxicity against LoVo cell line and *in vivo* antitumor efficacy in hepatic H22-bearing mice model through i.p. administration. Furthermore, the penetration of CDDP-loaded GEL-PAA nanoparticles through tumor tissue was assessed by observing the location of apoptotic cells caused by the released drug from the nanoparticles in relation to the tumor vasculature.

2. Materials and methods

2.1. Materials

Cisplatin (CDDP) was kindly provided by Jiangsu Hengrui Pharmaceutical Co., Ltd. (Lianyungang, China). Type-B gelatin with 100–115 mmol of carboxylic acid per 100 g of protein and an average molecular weight 40–50 kDa was purchased from Sigma–Aldrich (St. Louis, MO). The gelatin was refined once by dissolving it in distilled water followed by precipitating with acetone. The precipitate was then dried in a vacuum at room temperature for use later. Acrylic acid (AA) (Guanghua Chemical Company, Shanghai, China) was distilled under reduced pressure in nitrogen atmosphere. Potassium persulfate ($K_2S_2O_8$) was recrystallized from deionized water before use. 2,2′-(ethylenedioxy)bis(ethylamine), N-(3-dimethylaminopropyl)-N′-ethylcarbodiimide hydrochloride (EDC) and 1-(4,5-dimethylthiazol-2-yl)-3,5-diphenylformazan (MTT) were purchased from Aldrich. All other reagents were of analytical grade and used without further purification. Human colorectal cancer cell line LoVo and murine hepatic H22 cell line were purchased from Shanghai Institute of Cell Biology (Shanghai, China). Male ICR mice (6–8 weeks old) were purchased from Animal Center of Drum-Tower Hospital (Nanjing, China).

2.2. Preparation of GEL-PAA nanoparticles

Purified gelatin (0.8 g) was dissolved in 50 mL of acrylic acid (AA, 0.2 g) aqueous solution, and then the polymerization of AA monomer was initiated by $K_2S_2O_8$ at 80 °C. As the opalescence appeared in the reaction mixture, which was a signal to form gelatin-PAA nanoparticles, the reaction was allowed to proceed for another 120 min at 80 °C. The resultant suspension was then filtered with paper filter to remove any larger aggregation and dialyzed against a buffer solution of pH 3.0 for 24 h using a dialysis membrane bag (12 kDa cutoff) to remove residual monomers. After this, the cross-linking reaction of the nanoparticles was conducted by adding the desired amount of 2,2′-(ethylenedioxy)-bis(ethylamine) as cross-linker in the presence of EDC at room temperature for 12 h. The cross-linked product was again dialyzed against distilled water for 24 h.

2.3. Preparation of CDDP-loaded GEL-PAA nanoparticles

CDDP was dissolved in gelatin-PAA nanoparticle suspension (4.22 mg/mL) at 1 mg/mL, which was allowed to proceed at 37 °C for 2 days. And then, this suspension was treated with the method developed by Kataoka's group to remove free drug [22]. Briefly, the unbound CDDP was removed by dialysis against distilled water using a 12-kDa molecular weight cutoff dialysis membrane for 2 days. The Pt content in the nanoparticles was measured by ion-coupled plasma mass spectrometry (ICP-MS, Perkin-Elmer Corporation, USA).

2.4. Characterization of nanoparticles

2.4.1. Size and zeta potential analysis of the nanoparticles

The mean diameter and size distribution of nanoparticles were measured by dynamic light scattering (DLS) with a Brookheaven BI9000AT system (Brookheaven Instruments Corporation, USA). Zeta potential was measured by Zetaplus (Brookheaven Instruments Corporation, USA). All DLS measurements were done with a wavelength of 658.0 nm.

2.4.2. Transmission electron microscopy (TEM) and atomic force microscopy (AFM)

Transmission electron microscopy (TEM; JEOL TEM-100) observations were conducted to determine the morphology of cross-linked GEL-PAA nanoparticles. The solution of particles was dripped onto nitrocellulose-covered copper grid at room temperature without staining. Atomic force microscopy (AFM; SPI3800, Seiko Instruments, Japan) was also exploited to investigate the surface morphology of the nanoparticles in a greater detail. The sample with one drop of properly diluted suspension of particles was dripped onto the surface of a clean silicon wafer and dried under nitrogen flow at room temperature. The AFM observation was carried out with a 20 μm scanner in tapping mode.

2.4.3. Drug loading content and encapsulation efficiency

CDDP loading content was determined by ICP-MS. Briefly, the CDDP-loaded GEL-PAA nanoparticles were decomposed on heating in nitric acid. After being evaporated to dryness, they were dissolved in 2 N hydrochloric acid solution. Then, the Pt concentration in the solution was measured by ICP-MS. The following equations were used to evaluate the drug loading content and encapsulation efficiency.

$$\text{Drug loading content}\% = \frac{\text{Weight of the drug in nanoparticles}}{\text{Weight of the nanoparticles}} \times 100\%$$

$$\text{Encapsulation}\% = \frac{\text{Weight of the drug in nanoparticles}}{\text{Weight of the feeding drug}} \times 100\%$$

2.5. In vitro CDDP release from the nanoparticles

The release profile of CDDP from GEL-PAA nanoparticles in phosphate-buffered saline (PBS) at 37 °C was assessed by the dialysis method as previously reported [23]. Briefly, a purified CDDP-loaded nanoparticle solution of known platinum drug concentration was placed inside a dialysis bag (MWCO, 12000) and dialyzed against PBS (0.01 M phosphate buffer, pH 7.4, plus 0.15 M NaCl) at 37 °C. The released Pt outside of the dialysis bag was sampled at defined time periods and measured by ICP-MS.

2.6. Kinetic stability of CDDP-loaded nanoparticles in PBS

The kinetic stability of CDDP-loaded nanoparticles in PBS at 37 °C was measured by DLS with a Brookheaven BI9000AT system. Changes in the relative light scattering intensity and average hydrodynamic diameter of nanoparticles were evaluated at a defined time period.

2.7. In vitro cytotoxicity of CDDP-loaded nanoparticles

Cytotoxicity of CDDP-loaded nanoparticles against human colorectal cancer cell line LoVo was evaluated by MTT assay as previously described [24]. LoVo cells were seeded on 96-well plates with a density around 5000 cells/well and allowed to adhere for 24 h prior to the assay. Then, the cells were co-incubated with a series of doses of free CDDP, empty nanoparticles, and CDDP-loaded nanoparticles at 37 °C for 48 h. Thereafter, 50 μL of MTT indicator dye (5 mg/mL in PBS, pH 7.4) was added to each well, and the cells were incubated for another 2 h at 37 °C in the dark. The medium was withdrawn, and 200 μL of acidified isopropanol (0.33 mL HCl in 100 mL isopropanol) was added in each well to dissolve the crystals of dye. The solution was transferred to 96-well plates and immediately monitored on a microplate reader (Bio-Rad, Hercules, CA, USA). Absorption was measured at a wavelength of 490 nm and 620 nm as reference wavelength. The values measured were expressed as a percentage of the control cells to which no drugs were added.

2.8. In vivo antitumor efficacy of CDDP-loaded nanoparticles

All animal studies were performed in compliance with guidelines set by the Animal Care Committee at Drum-Tower Hospital. H22 cells ($4–6 \times 10^6$ cells per mouse) were inoculated subcutaneously to ICR mice (average body weight of 25 g) at the right axilla. When the tumor volume reached about 500 mm^3, the mice were selected, and this day was designated as Day 1. On Day 1, the mice were randomly divided into five groups, and each group was composed of 6 mice. Tumor-bearing mice were injected i.p. with saline, empty GEL-PAA nanoparticles, free CDDP (3 mg/kg), or CDDP-loaded nanoparticles (3 mg/kg CDDP eq. and 6 mg/kg CDDP eq.). The tumor volumes were measured every other day using calipers for 15 days. The tumor volume was calculated as $D \times d^2/2$, where D was the longest and d the shortest diameter. Moreover, the survival rates were also monitored throughout the study.

2.9. Histology observation

The tumor tissues of the mice that received saline, empty nanoparticles, free CDDP (3 mg/kg) and CDDP-loaded nanoparticles (3 mg/kg CDDP eq. and 6 mg/kg CDDP eq.) were selected for histology observation on the 15th day after treatment ($n = 3$ mice per group). The tumors were dissected and fixed in 10% neutral buffered formalin. Thereafter, the tissues were processed routinely into paraffin, sectioned at a thickness of 4 μm and stained with hematoxylin and eosin (H and E). The slices obtained were examined by optical microscopy.

2.10. Penetration in tumor tissue: imaging and staining of tumor slices

Tumors were taken from saline, empty nanoparticles and CDDP-loaded nanoparticles (6 mg/kg CDDP eq.) groups at 2 d post-administration. For staining of tissue sections, frozen sections (6 μm) were immunostained with polyclonal antibody against cleaved caspase-3 (Asp175, Cell Signaling Technology), monoclonal antibody against platelet/endothelial cell adhesion molecule 1 (PECAM-1; PharMingen) and TOPRO-3 (Molecular Probes). Alexa 488-conjugated and Alexa 594-conjugated anti-rabbit antibodies were used as secondary antibodies (Molecular Probes). Fluorescence signals were detected with a Zeiss LSM510 confocal microscope.

2.11. Statistical analysis

Quantitative data were expressed as mean ± SD. Statistical comparisons were made by ANOVA analysis and Student's t-test. P value <0.05 was considered statistically significant.

3. Results and discussion

3.1. Preparation and characteristics of CDDP-loaded GEL-PAA nanoparticles

In our previous work, we have introduced a simple and direct approach to prepare biocompatible nanoparticles by polymerizing monomer in a biopolymer–monomer pair reaction system consisting of the biopolymer and the polymerisable monomer [25,26]. In this study, we chose a reaction system in aqueous solution consisting of a cationic biomacromolecule, gelatin (GEL) and an anionic monomer, acrylic acid (AA). The GEL-PAA nanoparticles were synthesized by direct polymerization of AA monomers without any aid of organic solvents or surfactants. With the polymerization of the AA monomers, the electrostatic interaction between gelatin and AA turns into a stronger one between two oppositely charged polyions. When polymerization reaches a certain degree, the stable GEL-PAA nanoparticles are formed. Interestingly, the fact that zeta potential of the GEL-PAA nanoparticles is positive (20.1 mV) at pH about 3 at the end of the reaction while it experiences a reverse to negative value (−37.0 mV) upon an increase in pH to 7.4 indicates the surface charge switch property of GEL-PAA nanoparticles in response to the change of medium pH. Since type-B gelatin utilized in present case has an isoelectric point (pI) between 4.8 and 5.0 [20], we infer the microscopic structure of GEL-PAA nanoparticles with cationic gelatin corresponding to ionized amino groups (pH < pI) or anionic one with ionized carboxyl groups (pH > pI) as the shell to stabilizing the nanoparticles and GEL-PAA interpolyelectrolyte complex as the core. Further, the GEL-PAA nanoparticles were cross-linked using 2,2′-(ethylenedioxy)bis(ethylamine) in the presence of EDC to get more stable structure (Scheme 1). Fig. 1 shows the TEM and AFM images of as-obtained cross-linked GEL-PAA nanoparticles. From TEM image, it can be observed that the nanoparticles have a smaller size (about 100 nm) than that of measured by DLS (about 140 nm, Table 1) owing to the dry state. Additionally, AFM micrograph demonstrates that all the particles have a spherical shape.

Considering that the GEL-PAA particles are full of carboxyl groups in the gelatin and PAA molecules, they seem to be very appropriate to be the carriers for CDDP delivery since many works

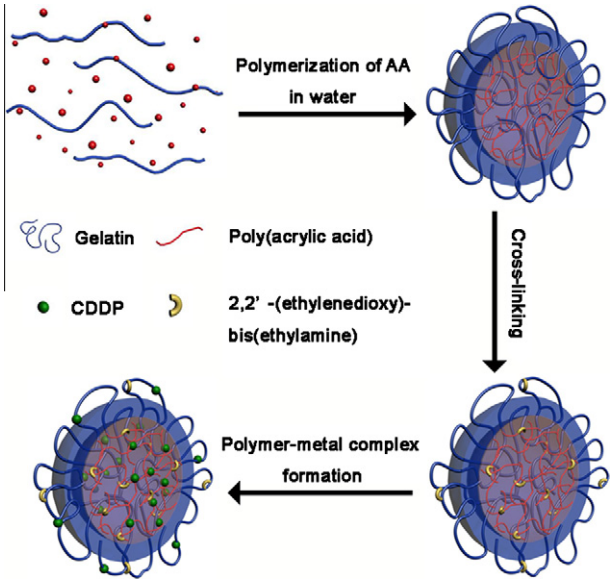

Scheme 1. Schematic illustration of the formation of CDDP-loaded GEL-PAA nanoparticles. (For interpretation of the references to color in this figure legend, the reader is referred to the web version of this article.)

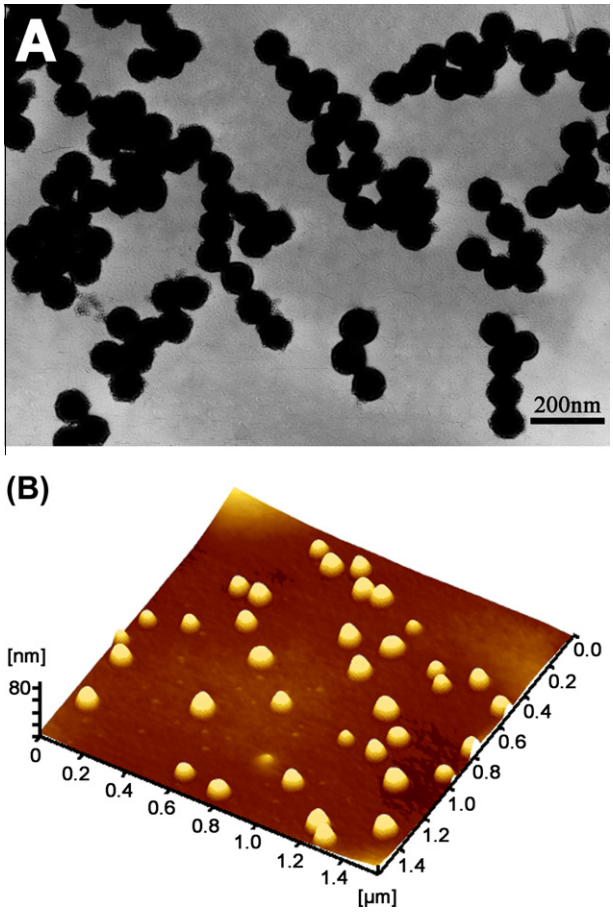

Fig. 1. TEM (A) and AFM (B) images of cross-linked GEL-PAA nanoparticles. (For interpretation of the references to color in this figure legend, the reader is referred to the web version of this article.)

Table 1
Characteristics of CDDP-loaded GEL-PAA nanoparticles.

CDDP feeding ([CDDP]/[COOH]) molar ratio	Diameter[a] (nm)/PDI[b]	D.L.[c] (%)	E.E.[d] (%)
0	142/0.14	NA	NA
1:1	95/0.12	39.9 ± 1.4	70.1 ± 3.9
1:3	102/0.12	20.0 ± 0.7	79.0 ± 3.5
1:5	120/0.12	12.5 ± 0.8	75.5 ± 5.5

[a] Mean diameter in PBS (pH 7.4) measured by DLS (n = 3).
[b] PDI = Polydispersity index.
[c] D.L. = Drug loading content.
[d] E.E. = Encapsulation efficiency. pH value in drug loading is around 6.

have indicated the polymer containing carboxyl groups can form polymer–metal complex with CDDP molecule [7,27]. Consequently, we successfully encapsulated CDDP into the GEL-PAA nanoparticles by the interaction between platinum of CDDP and carboxyl groups in the nanoparticles (Scheme 1). The physical properties of these CDDP-loaded nanoparticles with different CDDP feeding ratio were evaluated and listed in Table 1. The drug loading content of CDDP into GEL-PAA nanoparticles is substantially influenced by the molar ratio of CDDP to the carboxylic group of the nanoparticles and increases significantly from 12% to 40% by varying the drug feeding ratio. All of them have a relatively high encapsulation efficiency of more than 70%. The large amount of carboxylic groups in GEL-PAA nanoparticles should be responsible for the high drug loading content and encapsulation efficiency. In addition, it is also notable that the introduction of CDDP into GEL-PAA nanoparticles results in a decrease in average hydrodynamic diameter of nanoparticles, as detected by DLS measurement, suggesting that the interaction between platinum of CDDP and carboxylic group of nanoparticles further solidifies and contracts the nanoparticles. Furthermore, all of the samples have relatively narrow size distribution (polydispersity <0.15). These results verify that the CDDP-loaded GEL-PAA nanoparticles possess high drug loading content and encapsulation efficiency with appropriate size. In the next *in vitro* and *in vivo* experiments, the GEL-PAA nanoparticles with CDDP payload of 20% corresponding to [CDDP]/[COOH] = 1:3 in Table 1 were selected due to their relatively satisfying properties.

3.2. In vitro release of CDDP-loaded nanoparticles

For the release of CDDP from nanoparticles, as reported by Kataoka et al., the presence of chloride ions in media is essential for the release process since CDDP can be released by exchange reaction between chloride ions and carboxylic groups of nanoparticles [22]. Fig. 2 shows the release profile of CDDP from CDDP-loaded GEL-PAA nanoparticles at 37 °C in PBS. It can be seen that a very small initial burst with only about 13% of the total loaded amount is shown in the first 6 h, which may be ascribed to the strong interaction between CDDP and polymeric nanoparticles. Since the CDDP diffuses out of the nanoparticles after chloride ions cleaving the bonds between the drug and particles, the mechanism for CDDP release is quite different from that of physically encapsulating drugs which has a much larger initial burst from the nanoparticles [18]. After the initial stage, the CDDP-loaded nanoparticles release the drug in a sustained way. About 55% of the entrapped CDDP are released from the nanoparticles in 5 d. This result suggests that CDDP-loaded GEL-PAA nanoparticles show a continuous and slow release behavior for CDDP.

3.3. Kinetic stability of CDDP-loaded nanoparticles

The kinetic stability in biological media is an essential property of drug nanocarriers. The elevated stability of the drug-loaded particles may improve their blood circulation time [27]. The changes in the relative light scattering intensity and average hydrodynamic diameter of CDDP-loaded GEL-PAA nanoparticles in PBS at 37 °C and pH 7.4 are monitored by DLS and shown in Fig. 3. Although the relative scattering intensity of the sample decreases slightly in the period of 10 days, which may come from the release of

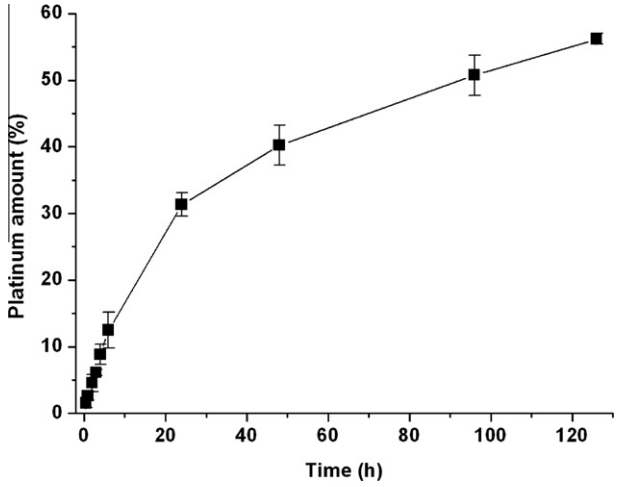

Fig. 2. *In vitro* release profile of CDDP from the GEL-PAA nanoparticles in PBS at 37 °C.

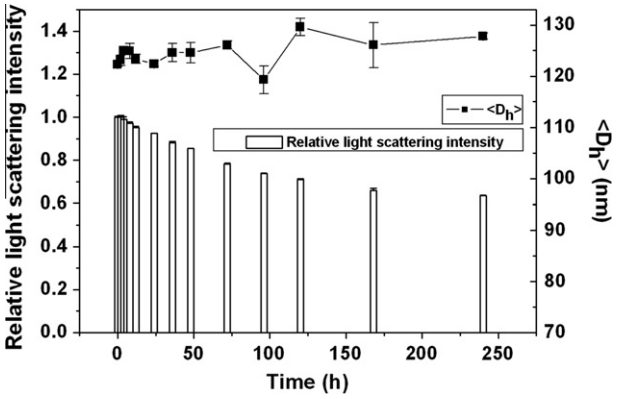

Fig. 3. The stability of CDDP-loaded GEL-PAA nanoparticles in PBS at 37 °C. The average hydrodynamic diameter (square) and relative light scattering intensity (column) of CDDP-loaded nanoparticles as functions of time.

loaded CDDP, the size of the nanoparticles is hardly changed even after 10 days, exhibiting a satisfactory stability. This result is similar to that of dichloro(1,2-diaminocyclohexane)platinum-loaded poly(ethylene glycol)–poly(glutamic acid) nanoparticles which have been demonstrated to be very suitable for systemic drug delivery [27]. Hence, our CDDP-loaded GEL-PAA nanoparticles seem to be very promising vehicles for further *in vivo* drug delivery.

3.4. In vitro cellular cytotoxicity of CDDP-loaded nanoparticles

To trace the cellular uptake of CDDP-loaded nanoparticles, the CDDP-loaded GEL-PAA nanoparticles were labeled with rhodamine B isothiocyanate (RBITC). The laser scanning confocal microscopy (LSCM) image was taken from MKN-28 cells co-incubated with RBITC-labeled nanoparticles at 37 °C for 2 h. As displayed in Fig. 4, the red fluorescence of labeled nanoparticles from the cell organelles and blue fluorescence of Hoechst 33258 from the nucleus indicate that GEL-PAA nanoparticles are mainly distributed in the entire cell cytoplasm and not in the nucleus, suggesting that the CDDP-loaded nanoparticles are able to penetrate cell membrane barriers.

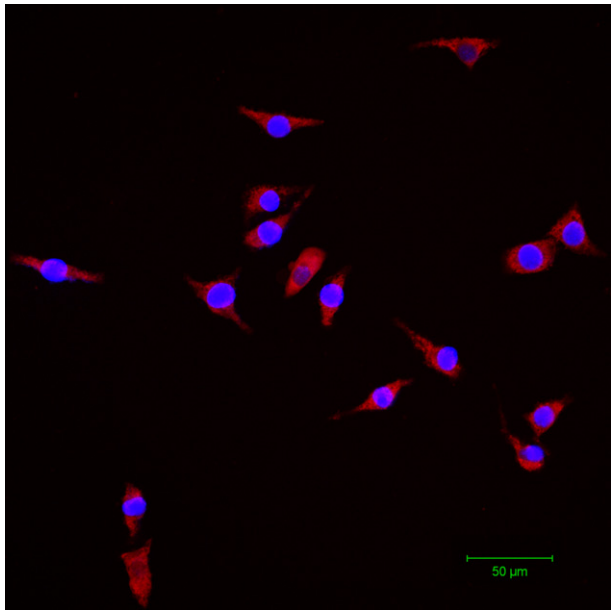

Fig. 4. Fluorescence confocal microscopy image of MKN-28 cells incubated with 25 μg/mL of CDDP-loaded nanoparticles labeled with RBITC at 37 °C for 2 h. The cell nuclei were stained by Hoechst 33258 (blue). (For interpretation of the references to color in this figure legend, the reader is referred to the web version of this article.)

Additionally, to examine the pharmacological activity of CDDP-loaded GEL-PAA nanoparticles, and to verify the cytotoxicity of these nanoparticles, the *in vitro* cytotoxicity tests of drug-loaded and empty nanoparticles against LoVo cell line were conducted. As seen in Fig. 5A, the inhibitory ratio was examined after 48 h of incubation with a series of doses of free CDDP and CDDP-loaded particles by MTT assay. The cytotoxicity of CDDP-loaded nanoparticles is slightly lower than that of free CDDP in the tested concentrations. Although the CDDP-loaded nanoparticles were incubated in cells for 48 h, it seems that the nanoparticles have not released enough CDDP causing the higher cytotoxicity than free drug. In addition, no significant cytotoxicity is observed with empty nanoparticles at all tested concentrations (Fig. 5B), suggesting that the empty GEL-PAA nanoparticles are no cytotoxicity at the normal concentration and show good biocompatibility.

3.5. In vivo antitumor efficacy of CDDP-loaded nanoparticles

Liver cancer is one of the most harmful forms of cancer, which is also a significant threat to the public health in China [28]. In the present study, mice implanted with murine hepatoma cell line H22 were used to study the antitumor efficacy of CDDP-loaded GEL-PAA nanoparticles. Intraperitoneal (i.p.) injection as a pathway

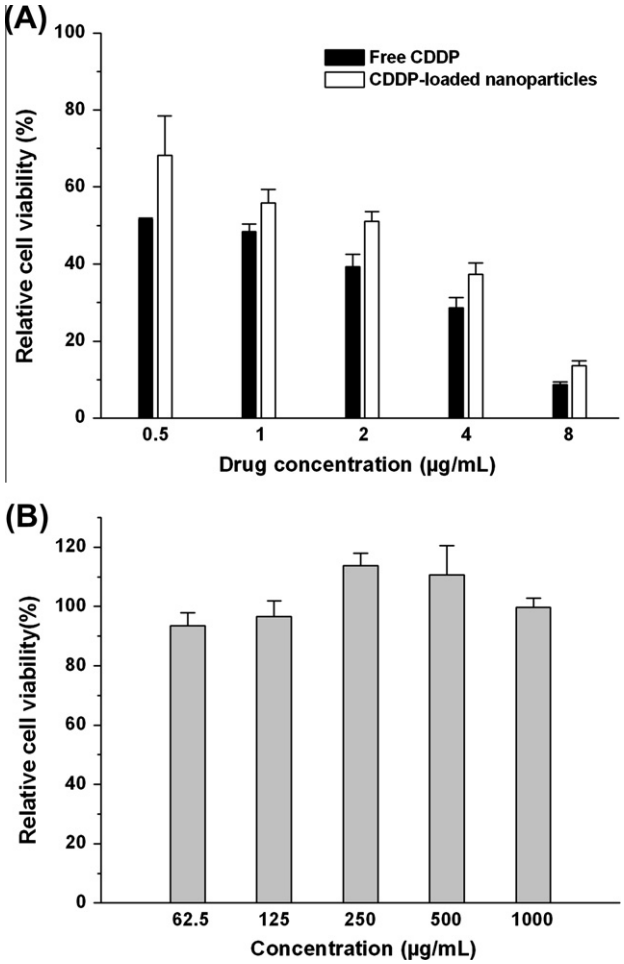

Fig. 5. (A) *In vitro* cytotoxicity of free CDDP and CDDP-loaded nanoparticles against LoVo cells after co-incubation for 48 h. (B) *In vitro* cytotoxicity of empty GEL-PAA nanoparticles against LoVo cells after co-incubation for 48 h.

for systemic delivery was administrated, and the anticancer effect between CDDP-loaded nanoparticles and free CDDP was compared. The treatments were done by i.p. injecting saline, empty GEL-PAA nanoparticles, free CDDP (3 mg/kg) or CDDP-loaded nanoparticles (3 mg/kg CDDP eq. and 6 mg/kg CDDP eq.), respectively, into tumor-bearing mice.

Fig. 6A depicts that neither saline nor empty GEL-PAA nanoparticles treatment has any effect on the tumor inhibition. Tumor volumes of the mice in both groups increased rapidly during the 15-day duration with their mean volumes reaching more than 8500 mm^3 on day 15. In contrast, the treatment of CDDP-loaded GEL-PAA nanoparticles effectively suppresses the tumor growth and displays a dose-dependent efficacy. The drug-loaded nanoparticle treatments at a dosage of 3 mg/kg CDDP equiv and 6 mg/kg CDDP equiv result in a significantly decreased tumor volume, that is, 5117.2 ± 703.9 mm^3 and 2543.2 ± 666.4 mm^3, respectively, at the termination of the experiment. The differences in tumor size between the nanoparticle groups (two doses) and saline group are highly significant (both $P < 0.01$). Moreover, the nanoparticle formulation exhibits much superior antitumor efficacy *in vivo* than free drug at the same CDDP dose of 3 mg/kg ($P < 0.05$ from day 7). Our results are quite different from ones that Li et al. and Xu et al. reported. Both found that the physical encapsulated CDDP in poly(ethylene glycol)–b-polycaprolactone (PEG–PCL) nanoparticles exhibited no advantage over free CDDP in two different tumor models through i.p. administration [18,29]. Physical encapsulation of drugs into PEG-PCL nanoparticles might result in the rapid release of CDDP from the nanocarriers *in vivo*. Hence, nanoparticle formulation showed similar efficacy with free CDDP by the systemic injection, which is quite different from our case with the formation of polymer–metal complex between CDDP and the nanoparticles. In the present study, the tumor inhibition rates on the 15th day post-administration confirm the dramatic antitumor efficacy of GEL-PAA nanoparticulate formulation as well. The inhibition rates of groups treated with the nanoparticles at the doses of 3 and 6 mg/kg CDDP equiv are 46.7% and 73.5%, respectively, compared with 32.2% of the group treated with CDDP injection (3 mg/kg). Additionally, it is also calculated that empty particles have negligible inhibition effect on tumor growth.

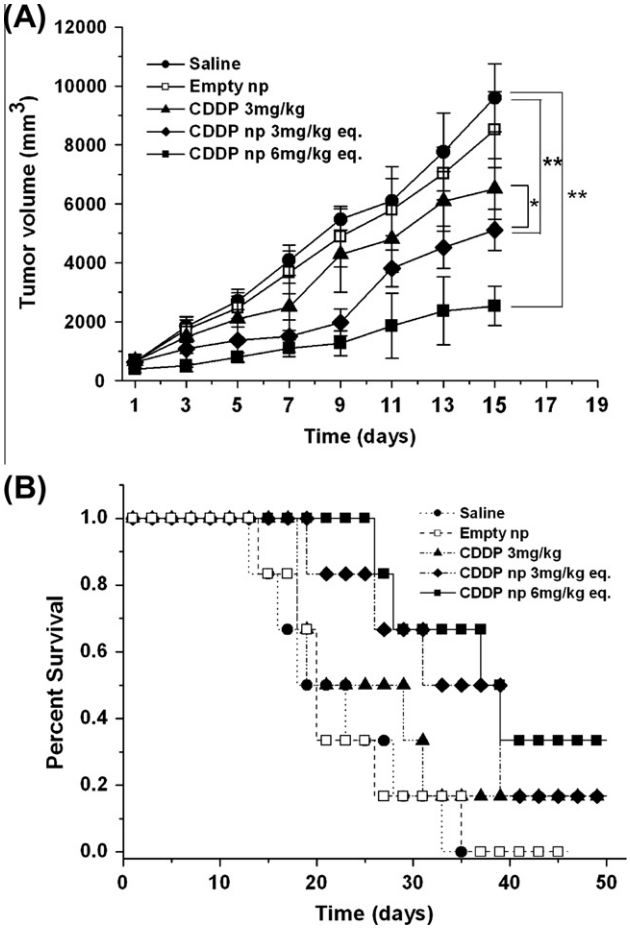

Fig. 6. Antitumor effect of CDDP-loaded nanoparticles in H22 (murine hepatoma cancer cell line) subcutaneous mouse model. (A) *In vivo* tumor volumes in various groups indicated after i.p. injection. * Represents $P < 0.05$ since the 7th day and ** Represents $P < 0.01$ since the 5th day. Data are presented as mean ± SD ($n = 6$). (B) Kaplan–Meier curves showing survival of tumor-bearing mice in each treated group.

Fig. 6B shows the survival rates of tumor-bearing mice in each treatment group. All of the mice treated with saline and empty nanoparticles died within 36 days owing to the significantly fast growth of H22 transplant tumor [28]. After the i.p. injection of free CDDP, only one animal survived for 32 days. On the contrary, in the groups receiving the nanoparticle formulation, half of the mice survived for 39 days although 5 and 4 of 6 mice died in nanoparticles-treated groups (3 and 6 mg/kg CDDP equiv, respectively) during the 50-day duration. The median survival time for the groups receiving saline, empty nanoparticles, free CDDP and CDDP-loaded nanoparticles at a dosage of 3 and 6 mg/kg CDDP equiv is 19, 21, 20, 32 and 38 days, respectively, suggesting that the survival rates of tumor-bearing mice treated with the nanoparticles are significantly improved, which may result from their superior antitumor effect and reduced side effect.

Next, we performed histological staining of the excised tumors from the mice of the experimental groups after 15 day post-injection. Hematoxylin and eosin (H and E) sections of tumors were examined by optical microscopy. As shown in Fig. 7, a large amount of living cells are able to be seen in the tumors from the mice treated with saline and empty nanoparticles. On the other hand, qualitatively, the existence of large area of necrotic region in the tumors from the mice treated with both the nanoparticle formulations suggests the much higher necrotic rate in contrast to that of other groups. These results corroborate the notably enhanced anticancer efficacy of CDDP-loaded nanoparticles once more.

As is well known to all, drug-encapsulated nanoparticles have the ability to achieve passive targeting so as to improve drug delivery to tumors through EPR effect when administered systemically (i.v. and i.p.) [30]. Moreover, more drugs can enter the interior of cells with the help of nanocarriers, which is crucial to exert the pharmacological activity of drug more efficiently [31]. In our case, the superior antitumor effect of CDDP-loaded GEL-PAA nanoparticles may associate with the factors mentioned earlier. In particular, compared with pure gelatin nanoparticles synthesized by desolvation [17], the PAA chains in the interior part of the GEL-PAA nanoparticles provide a large amount of carboxylic groups, leading to more CDDP incorporating into the nanoparticles in the form of polymer–metal complex and greatly enhancing the drug loading content as well as slow drug release behavior. This may be another reason for the improving antitumor efficacy of the nanoparticles. Additionally, the nanoparticles acting as drug concentrators possess relatively high kinetic stability, which probably signify long circulation time *in vivo*, benefiting the exertion of EPR effect of polymeric nanoparticles. This part of work will be investigated in detail in the future.

3.6. Penetration of CDDP-loaded nanoparticles in tumors

After injected intraperitoneally, the CDDP-loaded nanoparticles are able to enter into circulation system from peritoneum. Then

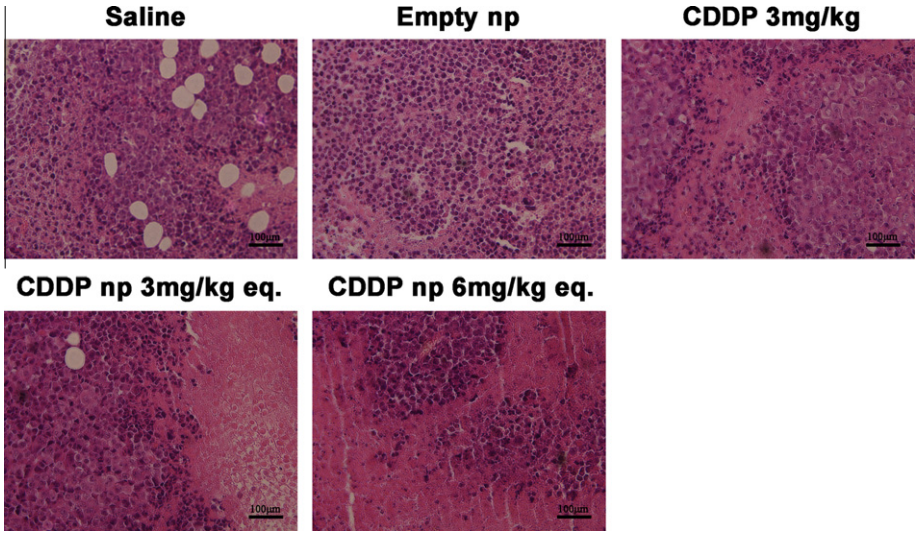

Fig. 7. H and E stained tumor slices from mice on the 15th day in various groups. (For interpretation of the references to color in this figure legend, the reader is referred to the web version of this article.)

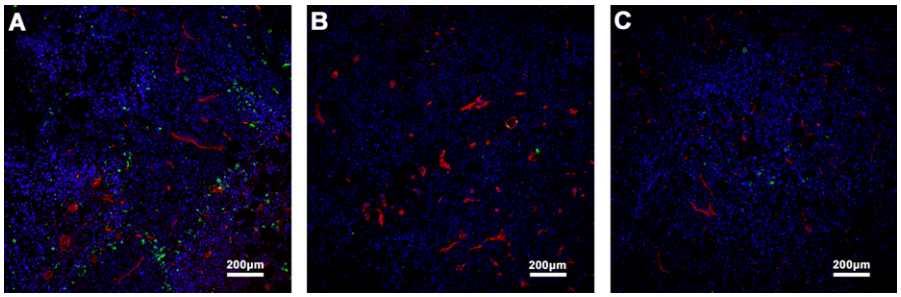

Fig. 8. Penetration of CDDP-loaded nanoparticles in tumors. Cleaved caspase-3 (apoptosis assay, green), PECAM-1 (blood vessels, red) and TOPRO-3 (nuclear, Blue) co-staining images of H22 tumor sections from mice receiving CDDP-loaded nanoparticles (6 mg/kg CDDP eq.) (A), saline (B) and empty nanoparticles (C), respectively. Tumors were taken from each treated group at 2 d post-administration. (For interpretation of the references to color in this figure legend, the reader is referred to the web version of this article.)

the nanoparticles tend to preferentially localize and accumulate in tumors via EPR effect [32]. Several studies demonstrated that nanocarriers could passively extravasate through the leaky vasculature, which is characteristic of solid tumors [33,34]. However, Jain et al. suggested that liposome nanoparticles with 90 nm in diameter could leak through the tumor vessels but were not able to penetrate any further within 10–20 μm away from the blood vessels after injected systemically [35]. To evaluate the penetration of CDDP-loaded GEL-PAA nanoparticles through tumor tissue, the tumors were taken from the mice and sectioned 2 days after i.p. administration of saline, empty nanoparticles and CDDP-loaded nanoparticles (6 mg/kg CDDP eq.). Then, the immunohistochemical staining was carried out to monitor the location of apoptotic cells relative to the vasculature. Fig. 8A indicates that cleaved caspase-3 positive cells (green fluorescence) of the tumors from the mice treated with CDDP-loaded nanoparticles, which represent the apoptosis in tumor, are distributed near the blood vessels (red fluorescence), whereas the region distant from the vessels contains barely detectable signals. Furthermore, cleaved caspase-3 positivity is hardly observed in tumors of mice receiving saline and empty nanoparticles (Fig. 8B and C), confirming the apoptosis resulting from the released CDDP from the GEL-PAA nanoparticles. This result suggests that the CDDP-loaded GEL-PAA nanoparticles with the size of about 100 nm have inability to effectively permeate the tumor deeply and affect the cells far from the vasculature after entering into the tumor, which is in good accordance with other reports [36,37]. This may be an important reason why the nanoparticle treatments via systemic injection are only able to impede tumor development efficiently but cannot eradicate the tumors completely.

4. Conclusions

In this study, CDDP-loaded GEL-PAA nanoparticles with high drug payload and stability were prepared. The CDDP-loaded nanoparticles have a mean size of about 100 nm. It is found that CDDP can be released from the nanoparticles in a sustained manner with a small initial burst release. The *in vitro* cytotoxicity of the nanoparticles is comparable to free CDDP after 48 h of co-incubation. The *in vivo* tumor inhibition measurements, survival rate examinations and histological staining experiments of tumor tissues demonstrate that the nanoparticle formulation has significantly superior anticancer efficacy in comparison with free drug and shows a dose-dependent effect. Moreover, the penetration tests of the nanoparticles through tumor reveal that the CDDP-loaded GEL-PAA nanoparticles can only affect the cells near the tumor vasculature after they enter into tumor tissue.

Acknowledgments

This work was supported by National Natural Science Foundation of China (Nos. 50625311, 20874042, and 51033002) and the New Drug Innovation Program of MOST (No. 2009ZX09503-028).

Thanks are given to Yulong He, Model Animal Research Institute, Nanjing University, for technical assistance in slices production and immunohistochemical examination.

References

[1] F. Gu, L.F. Zhang, B.A. Teply, N. Mann, A. Wang, A.F. Radovic-Moreno, R. Langer, O.C. Farokhzad, Precise engineering of targeted nanoparticles by using self-assembled biointegrated block copolymers, Proc. Natl. Acad. Sci. USA 105 (2008) 2586–2591.

[2] V. Torchilin, Multifunctional and stimuli-sensitive pharmaceutical nanocarriers, Eur. J. Pharm. Biopharm. 71 (2009) 431–444.

[3] J.H. Kim, Y.S. Kim, K. Park, E. Kang, S. Lee, H.Y. Nam, K. Kim, J.H. Park, D.Y. Chi, R.W. Park, I.S. Kim, K. Choi, I.C. Kwon, Self-assembled glycol chitosan nanoparticles for the sustained and prolonged delivery of antiangiogenic small peptide drugs in cancer therapy, Biomaterials 29 (2008) 1920–1930.

[4] F. Danhier, N. Magotteaux, B. Ucakar, N. Lecouturier, M. Brewster, V. Preat, Novel self-assembling PEG-p-(CL-co-TMC) polymeric micelles as safe and effective delivery system for Paclitaxel, Eur. J. Pharm. Biopharm. 73 (2009) 230–238.

[5] G. Mattheolabakis, E. Taoufik, S. Haralambous, M.L. Roberts, K. Avgoustakis, In vivo investigation of tolerance and antitumor activity of cisplatin-loaded PLGA-mPEG nanoparticles, Eur. J. Pharm. Biopharm. 71 (2009) 190–195.

[6] L. Nobs, F. Buchegger, R. Gurny, Current methods for attaching targeting ligands to liposomes and nanoparticles, J. Pharm. Sci. 93 (2004) 1980–1992.

[7] N. Nishiyama, S. Okazaki, H. Cabral, M. Miyamoto, Y. Kato, Y. Sugiyama, K. Nishio, Y. Matsumura, K. Kataoka, Novel cisplatin-incorporated polymeric micelles can eradicate solid tumors in mice, Cancer Res. 63 (2003) 8977–8983.

[8] S. Sengupta, D. Eavarone, I. Capila, G.L. Zhao, N. Watson, T. Kiziltepe, R. Sasisekharan, Temporal targeting of tumour cells and neovasculature with a nanoscale delivery system, Nature 436 (2005) 568–572.

[9] S.D. Li, L. Huang, Pharmacokinetics and biodistribution of nanoparticles, Mol. Pharm. 5 (2008) 496–504.

[10] M. Gaumet, A. Vargas, R. Gurny, F. Delie, Nanoparticles for drug delivery: the need for precision in reporting particle size parameters, Eur. J. Pharm. Biopharm. 69 (2008) 1–9.

[11] L.E. van Vlerken, Z. Duan, S.R. Little, M.V. Seiden, M.M. Amiji, Biodistribution and pharmacokinetic analysis of paclitaxel and ceramide administered in multifunctional polymer-blend nanoparticles in drug resistant breast cancer model, Mol. Pharm. 5 (2008) 516–526.

[12] S. Nagano, J.Y. Perentes, R.K. Jain, Y. Boucher, Cancer cell death enhances the penetration and efficacy of oncolytic herpes simplex virus in tumors, Cancer Res. 68 (2008) 3795–3802.

[13] T.T. Goodman, P.L. Olive, S.H. Pun, Increased nanoparticle penetration in collagenase-treated multicellular spheroids, Int. J. Nanomed. 2 (2007) 265–274.

[14] M.R. Dreher, W.G. Liu, C.R. Michelich, M.W. Dewhirst, F. Yuan, A. Chilkoti, Tumor vascular permeability, accumulation, and penetration of macromolecular drug carriers, J. Natl. Cancer Inst. 98 (2006) 335–344.

[15] M. Konishi, Y. Tabata, M. Kariya, A. Suzuki, M. Mandai, K. Nanbu, K. Takakura, S. Fujii, In vivo anti-tumor effect through the controlled release of cisplatin from biodegradable gelatin gydrogel, J. Control. Release 92 (2003) 301–313.

[16] J.H. Kim, Y.S. Kim, K. Park, S. Lee, H.Y. Nam, K.H. Min, H.G. Jo, J.H. Park, K. Choi, S.Y. Jeong, R.W. Park, I.S. Kim, K. Kim, I.C. Kwon, Antitumor efficacy of cisplatin-loaded glycol chitosan nanoparticles in tumor-bearing mice, J. Control. Release 127 (2008) 41–49.

[17] C.L. Tseng, W.Y. Su, K.C. Yen, K.C. Yang, F.H. Lin, The use of biotinylated-EGF-modified gelatin nanoparticle carrier to enhance cisplatin accumulation in cancerous lungs via inhalation, Biomaterials 30 (2009) 3476–3485.

[18] X.L. Li, R.T. Li, X.P. Qian, Y.T. Ding, Y.X. Tu, R. Guo, Y. Hu, X.Q. Jiang, W.H. Guo, B.R. Liu, Superior antitumor efficiency of cisplatin-loaded nanoparticles by intratumoral delivery with decreased tumor metabolism rate, Eur. J. Pharm. Biopharm. 70 (2008) 726–734.

[19] N. Nishiyama, Y. Kato, Y. Sugiyama, K. Kataoka, Cisplatin-loaded polymer–metal complex micelle with time-modulated decaying property as a novel drug delivery system, Pharm. Res. 18 (2001) 1035–1041.

[20] G. Kaul, M. Amiji, Long-circulation poly(ethylene glycol)-modified gelatin nanoparticles for intracellular delivery, Pharm. Res. 19 (2002) 1061–1067.

[21] H. Okino, R. Maeyama, T. Manabe, T. Matsuda, M. Tanaka, Trans-tissue, sustained release of gemcitabine from photocured gelatin gel inhibits the growth of heterotopic human pancreatic tumor in nude mice, Clin. Cancer Res. 9 (2003) 5786–5793.

[22] N. Nishiyama, M. Yokoyama, T. Aoyagi, T. Okano, Y. Sakurai, K. Kataoka, Preparation and characterization of self-assembled polymer–metal complex micelle from cis-dichlorodiammineplatinum(□) and poly(ethylene glycol)–poly(alpha, beta-aspartic acid) block copolymer in an aqueous medium, Langmuir 15 (1999) 377–383.

[23] Y. Chen, D. Ding, Z.Q. Mao, Y.F. He, Y. Hu, W. Wu, X.Q. Jiang, Synthesis of hydroxypropylcellulose-poly(acrylic acid) particles with semi-interpenetrating polymer network structure, Biomacromolecules 9 (2008) 2609–2614.

[24] R.T. Li, X.L. Li, L. Xie, D. Ding, Y. Hu, X.P. Qian, L.X. Yu, Y.T. Ding, X.Q. Jiang, B.R. Liu, Preparation and evaluation of PEG-PCL nanoparticles for local tetradrine delivery, Int. J. Pharm. 379 (2009) 158–166.

[25] Y.W. Zhang, Z.X. Wang, Y.S. Wang, H.X. Zhao, C.X. Wu, Facile preparation of pH-responsive gelatin-based core–shell polymeric nanoparticles at high concentrations via template polymerization, Polymer 48 (2007) 5639–5645.

[26] R. Guo, L.Y. Zhang, Z.P. Jiang, Y. Cao, Y. Ding, X.Q. Jiang, Synthesis of alginic acid-poly[2-(diethylamino)ethylmethacrylate] monodispersed nanoparticles by a polymer–monomer pair reaction system, Biomacromolecules 8 (2007) 843–850.

[27] H. Cabral, N. Nishiyama, S. Okazaki, H. Koyama, K. Kataoka, Preparation and biological properties of dichloro(1,2-diaminocyclohexane)platinum (□) (DACHPt)-loaded polymeric micelles, J. Control. Release 101 (2005) 223–232.

[28] Z.S. Zhu, Y. Li, X.L. Li, R.T. Li, Z.J. Jia, B.R. Liu, W.H. Guo, W. Wu, X.Q. Jiang, Paclitaxel-loaded poly(N-vinylpyrrolidone)-b-poly(ε-caprolactone) nanoparticles: preparation and antitumor activity in vivo, J. Control. Release 142 (2010) 438–446.

[29] P.S. Xu, E.A. Van Kirk, W.J. Murdoch, Y.H. Zhan, D.D. Isaak, M. Radosz, Y.Q. Shen, Anticancer efficacies of cisplatin-releasing pH-responsive nanoparticles, Biomacromolecules 7 (2006) 829–835.

[30] M. Morille, T. Montier, P. Legras, N. Carmoy, P. Brodin, B. Pitard, J.P. Benoit, C. Passirani, Long-circulating DNA lipid nanocapsules as new vector for passive tumor targeting, Biomaterials 31 (2010) 321–329.

[31] L.Y. Zhang, M. Yang, Q. Wang, Y. Li, R. Guo, X.Q. Jiang, C.Z. Yang, B.R. Liu, 10-Hydroxycamptothecin loaded nanoparticles: preparation and antitumor activity in mice, J. Control. Release 119 (2007) 153–162.

[32] O.C. Farokhzad, R. Langer, Impact of nanotechnology on drug delivery, ACS Nano 3 (2009) 16–20.

[33] Z. Liu, K. Chen, C. Davis, S. Sherlock, Q.Z. Cao, X.Y. Chen, H.J. Dai, Drug delivery with carbon nanotubes for in vivo cancer treatment, Cancer Res. 68 (2008) 6652–6660.

[34] K.Y. Kim, Nanotechnology platforms and physiological challenges for cancer therapeutics, Nanomed.: Nanotechnol. Biol. Med. 3 (2007) 103–110.

[35] F. Yuan, M. Leunig, S.K. Huang, D.A. Berk, D. Papahadjopoulos, R.K. Jain, Microvascular permeability and interstitial penetration of sterically stabilized (stealth) liposomes in a human tumor xenograft, Cancer Res. 54 (1994) 3352–3356.

[36] B. van Etten, T.L. ten Hagen, M.R. de Vries, G. Ambagtsheer, T. Huet, A.M. Eggermont, Prerequisites for effective adenovirus mediated gene therapy of colorectal liver metastases in the rat using an intracellular neutralizing antibody fragment to p21-Ras, Br. J. Cancer 86 (2002) 436–442.

[37] T.D. McKee, P. Grandi, W. Mok, G. Alexandrakis, N. Insin, J.P. Zimmer, M.G. Bawendi, Y. Boucher, X.O. Breakefield, R.K. Jain, Degradation of fibrillar collagen in a human melanoma xenograft improves the efficacy of an oncolytic herpes simplex virus vector, Cancer Res. 66 (2006) 2509–2513.